

## **INFLUENCE OF THE DEGREE OF DEHYDROXYLATION OF KAOLINITE ON THE PROPERTIES OF ALUMINOSILICATE GLASSES**

*H. Rahier<sup>1\*</sup>, B. Wullaert<sup>2</sup> and B. Van Mele<sup>1</sup>*

<sup>1</sup>Vrije University Brussels, Department for Physical Chemistry and Polymer Science, Pleinlaan 2  
1050 Brussels

<sup>2</sup>Present address: Indaver, 2030 Antwerp, Belgium

### **Abstract**

The degree of dehydroxylation of kaolinite,  $D_{TG}$  and  $D_{IR}$ , respectively, is characterized by thermogravimetric analysis (TG) and Fourier transform infrared spectroscopy (FTIR). The relation between  $D_{TG}$  and  $D_{IR}$  based on the infrared absorptions at 3600–3700, 915, 810, and 540  $\text{cm}^{-1}$  is established. Three regions can clearly be distinguished: the dehydroxylation region ( $D_{TG} < 0.9$ ), the metakaolinite region ( $0.9 < D_{TG} < 1$ ) and the 'spinel' region ( $D_{TG} = 1$ ). The effect of the degree of dehydroxylation of kaolinite on the amount of reactive material is measured by the reaction enthalpy,  $\Delta H$ , of the low-temperature reaction of the dehydroxylated kaolinite with a potassium silicate solution using differential scanning calorimetry (DSC).  $|\Delta H|$  increases almost linearly with  $D_{TG}$  in the dehydroxylation region. In the metakaolinite region,  $\Delta H$  and thus the amount of reactive material, becomes constant.  $|\Delta H|$  is sharply decreasing when metakaolinite transforms into other phases in the 'spinel' region. No significant differences in the reactivity of the dehydroxylates is detected with DSC. According to FTIR, the use of partially dehydroxylated kaolinite is not influencing the molecular structure of the low-temperature synthesized aluminosilicates, but residual kaolinite is retrieved as an additive.

**Keywords:** differential scanning calorimetry, FTIR, inorganic polymer glasses, kaolinite, metakaolinite, TG

### **Introduction**

The calcination or dehydroxylation process of clays has been studied extensively (e.g. [1–8]) in many cases for the direct use of the calcined clay as a material, or for the use of the thermally treated clay as a reactant. In previous work, it was shown that the low-temperature reaction between dehydroxylated kaolinite (Mk) and an aqueous silicate solution resulted in an amorphous aluminosilicate termed low-temperature inorganic polymer glass (LTIPG or IPG) with promising high-temperature and mechanical properties [9–11]. The degree of dehydroxylation of kaolinite, the resultant amount of reactive material and its reactivity are thus important parameters in the production of LTIPG.

\* Author for correspondence: Fax: 32/02/6293278, E-mail: hrahier@vub.ac.be

The dehydroxylation of kaolinite has been studied qualitatively and to some extent quantitatively by infrared spectroscopy (IR), infrared emission spectroscopy (IES) [8] and nuclear magnetic resonance spectroscopy (NMR) [1, 2]. IR absorption bands related to OH-vibrations, Al–O–H stretching bands in the region 3600–3700  $\text{cm}^{-1}$  (denoted as OH stretch) and the Al–O–H bending band at 915 with a shoulder at 938  $\text{cm}^{-1}$  (denoted as OH bend) gradually disappear during calcination and indicate a complete loss of OH groups at a degree of dehydroxylation of ca 80% (measured by the mass loss of water) [3, 4, 8]. Other changes in the structure related to the dehydroxylation process can be observed by IR too: the diminishing Al–O<sub>6</sub> octahedron stretching at 540  $\text{cm}^{-1}$  (denoted as Al<sup>VI</sup>) and the growing Al<sup>IV</sup>–O stretching band at 810  $\text{cm}^{-1}$  (denoted as Al<sup>IV</sup>) [3]. Due to the disordering of the structure the absorption bands broaden, which is clearly seen by disappearance of the fine-structure between 1000 and ca 1250  $\text{cm}^{-1}$ . A shoulder at about 1200  $\text{cm}^{-1}$  appears in this region.

In this paper, the use of dehydroxylated kaolinite as a reactant will further be studied.

The influence of the degree of dehydroxylation of kaolinite on this low-temperature reaction and on the final molecular structure of the synthesized aluminosilicate will be investigated.

For being able to understand the influence of the dehydroxylation on the low-temperature reaction, the structure of the dehydroxylated phase will be characterized via its degree of dehydroxylation, measured and quantified by both by TG and FTIR.

The amount of reactive material in the thermally treated kaolinite will then be determined by DSC via the reaction enthalpy of its low-temperature reaction with a potassium silicate solution. These DSC experiments will also give an indication on the reactivity of the different (partially) dehydroxylated kaolinites.

The effect of the degree of dehydroxylation of the clay on the structure of the synthesized aluminosilicate will be studied by FTIR.

## Materials and techniques

### *Materials*

The kaolinite used in this work was a well crystallized kaolin (KGa-1) [12], which was dehydroxylated in a preheated quartz crucible (the maximum height of the kaolinite bed was 10 mm) placed in a tube furnace in air. Three different series of dehydroxylates were prepared:

- (1) samples heated for 3 h at calcination temperatures between 150 and 1040°C;
- (2) samples heated at 500°C for calcination times between 5 and 4070 min;
- (3) samples heated at 600°C for calcination times between 5 and 900 min.

The amount of reactive material in the dehydroxylates was measured via the reaction with a potassium silicate solution, denoted as K-Sil, with composition in molar ratios:  $\text{SiO}_2/\text{K}_2\text{O}=1.7$ ;  $\text{H}_2\text{O}/\text{K}_2\text{O}=11.2$ .

DSC samples for the study of the low-temperature reaction were always freshly mixed.

LTIPG samples for structural analysis by FTIR were obtained by mixing the appropriate amount of K-Sil and Mk, and curing this mixture in a closed mold at room temperature for at least two days.

### *Techniques*

#### Thermogravimetric Analysis

The thermobalance used was a Perkin Elmer TG 7. The purge gas was He. To determine the total or residual bound water content of the samples, the following temperature program was used: the sample was dried at 250°C for 3 h [13], then the temperature was raised (at 50°C min<sup>-1</sup>) to 1000°C for 4 h and subsequently lowered to 250°C. Only the mass loss after drying was taken into account and baseline effects were minimized by comparing the masses at the same temperature (250°C). This procedure allowed accuracies of ±0.02 mass %.

#### Fourier transform infrared spectroscopy

IR spectra were obtained with a Perkin Elmer FTIR 1760 using KBr pellets (13 mm pellets with ca 1 mg sample/200 mg KBr). KBr and sample were mixed and ground in a 'Wig-L-Bug' for 3 min and dried overnight at 110°C before pressing the pellet. For each spectrum, 100 scans with a resolution of 4 cm<sup>-1</sup> were averaged.

#### Differential scanning calorimetry

DSC measurements were performed on a DSC 7 from Perkin Elmer. Reusable high pressure stainless steel sample pans were used. Scans were performed between -60 and 300°C at 5°C min<sup>-1</sup>.

## **Results and discussion**

### *Dehydroxylation process and degree of dehydroxylation*

The degree of dehydroxylation is quantified by TG and FTIR for the (partially) dehydroxylated kaolinites of series 1, 2, and 3, submitted to a different thermal treatment.

The residual mass loss measured with TG gives direct information on how much 'water' is retained in the partially dehydroxylated clay. The degree of dehydroxylation  $D_{TG}$ , obtained by TG, is calculated as:  $D_{TG} = 1 - m/m_0$ , where  $m$  and  $m_0$  is residual and maximum mass loss respectively (the maximum mass loss for the kaolinite used is 13.76 mass%).

Molecular structural changes during dehydroxylation are examined with FTIR. The areas of the following peaks (or groups of peaks) are calculated: 3700–3600, 915 (shoulder included), 810, and 540 cm<sup>-1</sup>. The peak areas are normalized against a reference band between 1300–960 cm<sup>-1</sup>. The structural changes during dehydroxylation are illustrated with the FTIR spectra of Fig. 1.

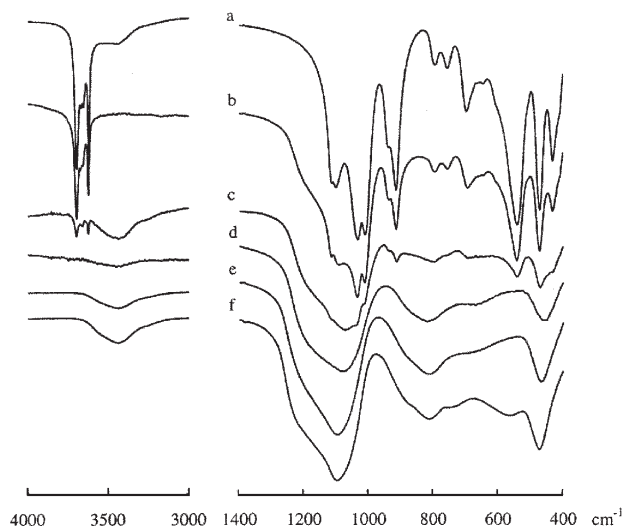


**Fig. 1** FTIR spectra of different dehydroxylated kaolinites ( $D_{TG}$ )  $a=0$ ;  $b=0.43$ ;  $c=0.71$ ;  $d=0.91$ ;  $e=0.99$  and  $f=1$

The degree of dehydroxylation  $D_{IR}$ , measured with FTIR, is calculated for diminishing absorption peaks at 3600–3700 (OH stretch), 915 (OH bend) and 540  $\text{cm}^{-1}$  ( $\text{Al}^{\text{VI}}$ ), as:  $D_{IR}=1-S/S_0$ , where  $S$  and  $S_0$  is peak area and maximum peak area respectively (the maximum peak area is the normalized peak area of the corresponding IR absorption *before* calcination).

For the growing absorption peak at 810  $\text{cm}^{-1}$  ( $\text{Al}^{\text{IV}}$ ) the degree of dehydroxylation  $D_{IR}$  was calculated as:  $D_{IR}=S/S_0$  (the maximum peak area  $S_0$  is the normalized peak area of the absorption at 810  $\text{cm}^{-1}$  *after* calcination during 3 h at 850°C).

An illustration is given in Fig. 2, where  $D_{TG}$  (Fig. 2a) and  $D_{IR}$  (Fig. 2b) are shown as a function of temperature for the dehydroxylates of series 1.

The calculation of the peak areas of the diminishing IR absorptions becomes impossible for high degrees of calcination ( $D_{TG}>0.80$ – $0.85$ ), so that from that moment on  $D_{IR}$  equals one. This is consistent with literature [3]. On the other hand, the growing peak at 810  $\text{cm}^{-1}$  can only be quantified if the degree of calcination is high enough ( $D_{TG}>0.70$ ). This implies that the peak area of the absorption at 810  $\text{cm}^{-1}$  is a good indication for high degrees of dehydroxylation, where the OH-related absorptions become too small to be measured.

Three regions can be distinguished (Fig. 2): (i) in the first, called here the dehydroxylation region, up to 550°C and  $D_{TG}$  0.85–0.9,  $D_{IR}$ (OH stretch, OH bend and  $\text{Al}^{\text{VI}}$ ) increases sharply to a value of one, consistent with the data from Frost *et al.* obtained from infrared emission spectroscopy [8]; (ii) in the second, called the Mk region, between 550 and 850–900°C for  $0.85$ – $0.9 < D_{TG} < 1$ , only  $D_{IR}$ ( $\text{Al}^{\text{IV}}$ ) can be calculated. Its value increases only slightly between 550 and 700°C, and above 700°C remains almost constant and

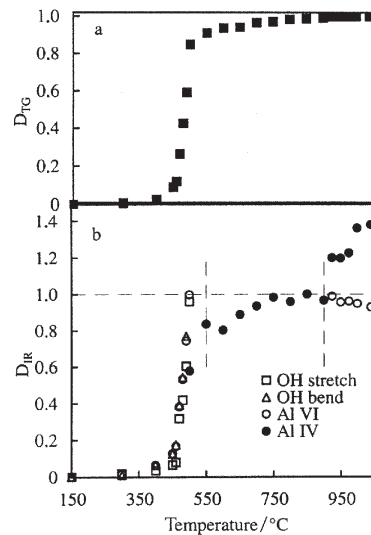


**Fig. 2** Degree of dehydroxylation of samples of series 1 as a function of the calcination temperature: a –  $D_{TG}$  and b –  $D_{IR}$ . The dehydroxylation region, Mk region and spinel region are separated by vertical dashed lines

equal to one. Note that  $D_{TG}$  values between  $\leq 0.85$ – $0.9$  and  $1$  are generally accepted to characterize Mk [5, 6]; (iii) above  $900^\circ\text{C}$  in the so called ‘spinel’ region, the  $\text{Al}^{\text{IV}}$  peak still increases and  $\text{Al}^{\text{VI}}$  reappears. It should be pointed out that because of the additional phase transformations involved in this region,  $D_{IR}(\text{Al}^{\text{IV}}$  and  $\text{Al}^{\text{VI}})$  should not be regarded any longer as a pure ‘degree of dehydroxylation’. Anyhow,  $D_{TG}$  can be considered as constant and equal to one in this region.  $D_{IR}$  for the different IR vibrations is plotted against  $D_{TG}$  in Fig. 3, a–d.

The relation between  $D_{IR}$  and  $D_{TG}$  is obvious, not only for the OH-related vibrations (Figs 3a and 3b) but also for the peaks at  $540\text{ cm}^{-1}$  ( $\text{Al}^{\text{VI}}$ ; Fig. 3c) and  $810\text{ cm}^{-1}$  ( $\text{Al}^{\text{IV}}$ ; Fig. 3d), although for  $\text{Al}^{\text{IV}}$  the correlation is different.  $D_{IR}(\text{OH stretch, OH bend, and Al}^{\text{VI}})$  predict total dehydroxylation or  $D_{IR}=1.0$  at a value for  $D_{TG}$  of ca  $0.8$ . This result is consistent with literature [3].

At first sight, one might expect a one to one relation between the decreasing concentration of OH-groups seen with FTIR and calculated from the residual mass loss by TG, as indicated by the dashed lines in Fig. 3. However, after 20% of dehydroxylation,  $D_{IR}(\text{OH stretch})$  increases faster than  $D_{TG}$ .  $D_{IR}(\text{OH bend})$  is immediately above the values of  $D_{TG}$ . This deviation gets more pronounced for  $D_{TG}>0.2$ . The same trend is observed for  $D_{IR}(\text{Al}^{\text{VI}})$ . For samples of series 1, 2 and 3 the same results are obtained, hence samples with the same  $D_{TG}$  will have the same molecular structure, independent of their thermal history. Since some peaks are broad and overlap and since the shape of the curves might depend on the possibly changing area of the IR reference band during calcination, care should be taken in discussing the shape of the curves of Fig. 3.

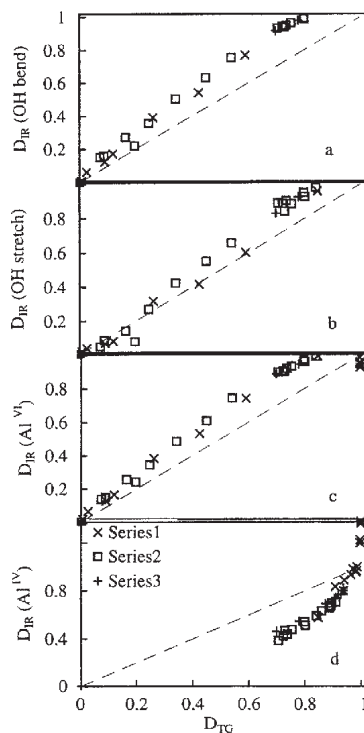


**Fig. 3** Degree of dehydroxylation measured with FTIR ( $D_{IR}$ ) as a function of the degree of dehydroxylation measured with TG ( $D_{TG}$ ) for samples of series 1, 2 and 3: a –  $D_{IR}(\text{OH bend})$ , b –  $D_{IR}(\text{OH stretch})$ , c –  $D_{IR}(\text{Al}^{\text{VI}})$ , and d –  $D_{IR}(\text{Al}^{\text{IV}})$ . The dashed lines indicate the one to one ratio between  $D_{IR}$  and  $D_{TG}$

Nevertheless, one can conclude that  $D_{IR}(\text{OH stretch, OH bend and Al}^{\text{VI}})$  tends faster to a complete dehydroxylation than expected from  $D_{TG}$ . The reason for this faster disappearance of OH related vibrations in IR, than the disappearance of OH itself in the form of water, can be looked for in the distortion of the regularity of the crystals upon calcination. Based on NMR results, Meinhold and coworkers concluded that OH-groups become related to different, sometimes distorted, Al sites other than the parent  $\text{Al}^{\text{VI}}$  [1]. Note that the NMR resonances for different Al sites also overlap, complicating quantification. The results of this work are consistent with these NMR findings, confirming that part of the OH-groups become related to different Al sites and that this process, at least for  $D_{IR}(\text{OH bend})$ , starts from the beginning of dehydroxylation. Indeed, the differentiation of OH-sites causes a peak broadening in IR, and some IR absorptions may disappear in the baseline. OH-groups not detected in IR for this reason are probably linked to distorted  $\text{Al}^{\text{VI}}$  sites or to Al-sites with different coordination. The similarity between  $D_{IR}(\text{OH bend})$  and  $D_{IR}(\text{Al}^{\text{VI}})$  (Fig. 3) indicates that the OH-groups still detected in IR are probably related to parent  $\text{Al}^{\text{VI}}$  sites.

*Amount of reactive material and reactivity of dehydroxylated kaolinite*

The low-temperature reaction between metakaolinite and an aqueous silicate solution results in an amorphous aluminosilicate termed inorganic polymer glass (IPG) [9, 10]. This low-temperature reaction was studied for a model system using meta-kaolinite, originating from the same kaolinite KGa-1 as in this study, with  $D_{TG}$  equal to 0.97 [9]. If the stoichiometric one to one molar mixing ratio of this ‘model Mk’ with the specific potassium silicate solution K-Sil of this work is obeyed, the reaction yields an amorphous potassium aluminosilicate or K-IPG in which all Al and Si of the reaction mixture is incorporated [11].

The influence of  $D_{TG}$  on this low-temperature reaction is studied in this section. The amount of reactive material formed during dehydroxylation of KGa-1 is measured with DSC via the low-temperature reaction enthalpy,  $\Delta H$ , of the thermally treated clay with K-Sil. The reactants were always mixed according to a molar ratio K-Sil/dehydroxylate of one to one [11]. Typical examples of DSC curves of non-isothermal experiments for dehydroxylates with different  $D_{TG}$  are given in Fig. 4.

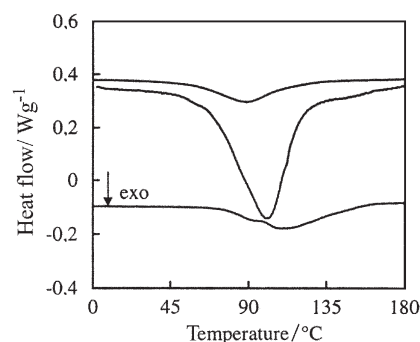


**Fig. 4** DSC curve of the low-temperature reaction of the potassium silicate solution with different dehydroxylated kaolinites: a –  $D_{TG}=0.20$  (dehydroxylation region), b –  $D_{TG}=0.94$  (Mk region) and c –  $D_{TG}=1.0$  (spinel region)

Note that Fig. 4b coincides with the DSC curve for the reaction of the ‘model Mk’ with K-Sil. Figure 5 shows that  $|\Delta H|$  increases sharply between 450 and 550°C and then, within the experimental error, a plateau for  $|\Delta H|$  is reached between 550 and 900°C.

At last, after calcination for 3 h at temperatures above 900°C,  $|\Delta H|$  sharply decreases again. Remark that the decrease in  $|\Delta H|$  coincides with the further increase of  $Al^{IV}$  and the reappearance of  $Al^{VI}$  in IR (Fig. 2b).

$|\Delta H|$  is determined by the degree of dehydroxylation rather than by the chosen thermal treatment during the calcination procedure, as illustrated in Fig. 6 for all the samples of series 1, 2 and 3.

$|\Delta H|$  increases with  $D_{TG}$  up to a value of  $D_{TG}$  equal to ca 0.85–0.90. This shows that the amount of reactive material increases with  $D_{TG}$  in the dehydroxylation region. For  $D_{TG}$  between 0.9 and 0.99 in the Mk region,  $|\Delta H|$  is not increasing anymore. For

$D_{TG}$  close or equal to one in the spinel region, a sharp decrease of  $|\Delta H|$  is again observed. Mk is transformed into other phases above 900°C [6], some of which will not react or at least via another reaction mechanism with the alkaline silicate solution, and others such as amorphous  $\text{SiO}_2$  will dissolve in the silicate solution. This can explain why the enthalpic content of the reaction exotherm becomes smaller, is shifted to higher temperatures, and why its shape is also different (compare the curves of Figs 4b and 4c).

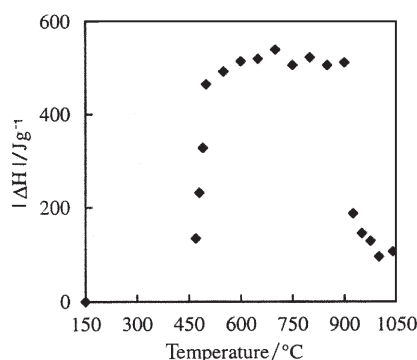


**Fig. 5** Reaction enthalpy  $|\Delta H|$  per gram dehydroxylate of the low-temperature reaction with the potassium silicate solution as a function of the calcination temperature of the dehydroxylated kaolinite (samples of series 1)

These DSC results also show the three different regions in the calcination process. In the dehydroxylation region,  $|\Delta H|$  and so the amount of reactive material increases. At the end, after the onset of spinel crystallization,  $|\Delta H|$  drops sharply. In between, in the Mk region,  $|\Delta H|$  reaches a plateau and here the amount of reactive material is high and remains almost constant. No pronounced maximum is found. These observations do not support the findings from Bachiorrini and Murat [14–16], who concluded that the structural changes introduced during further dehydroxylation in

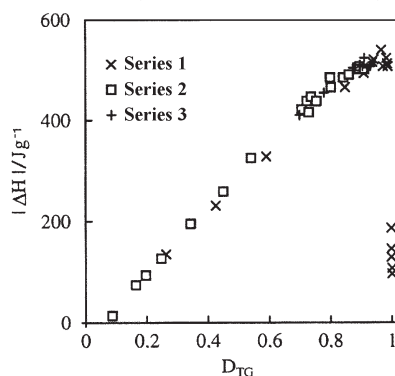


**Fig. 6** Reaction enthalpy  $|\Delta H|$  per gram dehydroxylate of the low-temperature reaction with the potassium silicate solution as a function of  $D_{TG}$  of the dehydroxylated kaolinite



the Mk region influence the 'reactivity'. It should be stressed that these authors measured another reaction (enthalpy of solution in hydrofluoric acid) in a calorimeter. From our DSC results, some conclusions on the reactivity of the dehydroxylated kaolinite can be made. An increase of the exothermic peak temperature from 79 to 101°C is observed for a dehydroxylate with  $D_{TG}=0.08$  to  $D_{TG}\geq 0.35$ , respectively, up to a maximum value of 105°C in the Mk region ( $D_{TG}>0.85-0.90$ ). At first sight, this would indicate that the reactivity decreases with increasing  $D_{TG}$ . The onset of the reaction exotherm, however, is constant at ca. 25°C (compare Fig. 4a and 4b) and the DSC signal of samples with lower  $D_{TG}$  is situated completely within the signal of samples with higher  $D_{TG}$ . This means that the reaction rate, proportional to the height of the DSC signal, and thus the reactivity at each temperature is higher for samples with higher  $D_{TG}$ . For samples with a value of  $D_{TG}$  between 0.85–0.90 and 0.99 (Mk region), no distinction can be made based on this type of DSC measurements. This leads to the conclusion that the DSC signal is not shifting to a higher temperature with higher  $D_{TG}$ , but that it is broadened, starting from the same temperature and extending to higher temperatures. The metakaolinite particles dehydroxylate in a layer by layer sequence in the first 70% of dehydroxylation [17]. If one assumes that this process starts from the outer layers of the particle, one can understand the evolution of the DSC curves with  $D_{TG}$ . The outer layers will react first with the alkaline solution, because the inner layers are not accessible at the beginning of the reaction. So, for higher degrees of dehydroxylation the reaction time with the silicate will be longer only because of mass transport phenomena.

A second conclusion is that, since the onset of the reaction is at a constant temperature, even in the Mk region one could argue that the reactivity of the outer layers is independent of the degree of dehydroxylation. The further elimination of remaining hydroxyl groups in Mk layers probably introduces only minor changes in the reactivity and in  $|\Delta H|$ . The error on the DSC signal and thus on  $|\Delta H|$  is probably too large for highlighting these small structural changes taking place in the Mk region. The apparent reactivity of Mk primarily depends upon other factors, such as particle size, obscuring the effect of small structural changes on the reactivity [18].

These DSC results do not indicate that the reactivity of the dehydroxylate is influenced to a large extent by  $D_{TG}$ . Only the amount of reactive material is increasing with the degree of dehydroxylation if  $D_{TG}<0.9$ .

#### *Influence of the degree of dehydroxylation on the structure of the inorganic polymer glass*

To investigate the influence of the calcination procedure on the properties of IPG, its molecular structure is investigated with FTIR as a function of the degree of dehydroxylation of the calcined clay.

For  $D_{TG}<0.9$  in the dehydroxylation region, absorptions of remaining kaolinite are seen in the FTIR spectrum (Figs 7a and 7b: e.g. sharp peaks in the region 3700–3600 and the peak at 540  $\text{cm}^{-1}$ ) in combination with the expected absorptions for IPG (Fig. 7: e. g. bands at 1020, 700 and 580  $\text{cm}^{-1}$  [11]).

The remaining kaolinite and unreacted Sil are to be considered as additives in the inorganic polymer glass. Specific absorptions of remaining Sil cannot be detected in the FTIR spectra because they overlap with absorptions of IPG or kaolinite, but it should be possible to detect the remaining Sil with NMR [9].

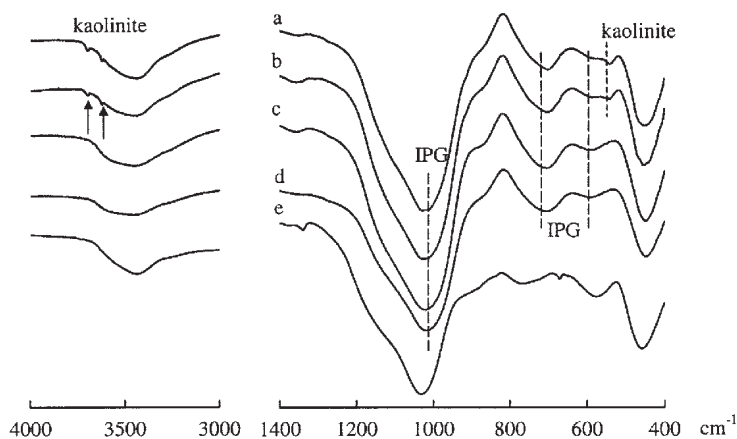


**Fig. 7** FTIR spectra of IPG prepared by the low-temperature reaction of the potassium silicate solution with different dehydroxylated kaolinites ( $D_{TG}$ );  $a=0.43$ ;  $b=0.71$ ;  $c=0.91$ ;  $d=0.99$  and  $e=1$

For  $D_{TG} > 0.9$  in the Mk region, no remaining kaolinite is detected in the FTIR spectrum of IPG and no changes in the spectrum over the entire Mk region are obvious (Figs 7c and 7d).

As previously mentioned, some phases of the spinel region will not react or at least via another reaction mechanism with the alkaline silicate solution, and others such as amorphous  $\text{SiO}_2$  will dissolve in the silicate solution. The reaction product formed in this case is not stable in water and its FTIR spectrum (Fig. 7e) is also different from the one for IPG, proving that the reaction nor the reaction product are comparable to those for Mk.

Generally, it can be concluded that samples in the Mk region lead to pure IPG. For samples with a smaller degree of dehydroxylation (in the dehydroxylation region), kaolinite is retrieved as an unreacted additive in IPG, which itself has apparently the same structure as if prepared from samples in the Mk region. These results are in line with the previous DSC results.

## Conclusions

In the temperature interval investigated, a dehydroxylation region, Mk region and spinel region are clearly distinguished by the degree of dehydroxylation, characterized with TG ( $D_{TG}$  calculated from the residual mass loss of water), FTIR ( $D_{IR}$  calculated from IR absorptions at 3600–3700, 915, 810, and 540  $\text{cm}^{-1}$ ) and DSC (via  $|\Delta H|$ ) of the low-temperature reaction of the calcined clay with a potassium silicate solu-

tion). The relation between  $D_{TG}$  and  $D_{IR}$  is demonstrated. However, IR spectroscopy offers more information on the molecular changes, useful in understanding the trend of  $|\Delta H|$  of the low-temperature reaction, especially in the case of phase transformations occurring at the end of the calcination process.

$|\Delta H|$  and thus the amount of reactive material increases linearly with  $D_{TG}$  in the dehydroxylation region. The reaction product is IPG and unreacted kaolinite is also retrieved. In the Mk region,  $|\Delta H|$  remains constant and the reaction product is IPG over the whole Mk region.  $|\Delta H|$  decreases from the start of the spinel transformation. From this point on, the reaction product is also different.

The reactivity of the dehydroxylate is at first approximation constant till the start of the spinel transformation, but other factors such as mass transport during reaction play an important role on the apparent reactivity. No evidence is found that the reactivity of the dehydroxylate is changing in the Mk region.

As a general conclusion, one can say that the amount of reactive material is at maximum in the Mk region from a  $D_{TG}$  value of 0.9 on, independent of the temperature of calcination. This does not imply, however, that the mechanical properties of the resulting IPG would be insensitive to small changes in the structure of the dehydroxylate, but here still other factors such as particle size distribution and density play a dominant role.

## References

- 1 R. H. Meinhold, R. C. T. Slade and T.W. Davies, *Appl. Magn. Reson.*, 4 (1993) 141.
- 2 J. Rocha and J. Klinowski, *Angew. Chem.*, 102 (1990) 539.
- 3 J. F. Lambert, W. S. Millman and J. J. Fripiat, *J. Am. Chem. Soc.*, 111 (1989) 3517.
- 4 R. C. T. Slade, T. W. Davies, H. Atakul, R. M. Hooper and D. J. Jones, *J. Mater. Sci.*, 27 (1992) 2490.
- 5 K. J. D. Mackenzie, I. W. M. Brown, R. H. Meinhold and M. E. Bowden, *J. Amer. Ceram. Soc.*, 68 (1985) 293.
- 6 I. W. M. Brown, K. J. D. Mackenzie, M. E. Bowden and R. H. Meinhold, *J. Amer. Ceram. Soc.*, 68 (1985) 298.
- 7 D. Massiot, P. Dion, J. F. Alcover and F. Bergaya, *J. Amer. Ceram. Soc.*, 78 (1995) 2940.
- 8 R. L. Frost and A. M. Vassallo, *Clays Clay Miner.*, 44 (1996) 635.
- 9 H. Rahier, B. Van Mele, M. Biesemans, J. Wastiels and X. Wu, *J. Mater. Sci.*, 31 (1996) 71.
- 10 H. Rahier, B. Van Mele and J. Wastiels, *J. Mater. Sci.*, 31 (1996) 80.
- 11 H. Rahier, W. Simons, B. Van Mele and M. Biesemans, *J. Mater. Sci.*, 32 (1997) 2237.
- 12 H. Van Olphen and J. J. Fripiat, *Data Handbook for Clay Materials and Other Non-Metallic Minerals*, Pergamon Press, London 1979.
- 13 D. Potzold, B. Poppe and T. Trager, *Silikattechnik*, 38 (1985) 352.
- 14 A. Bachiurrini and M. Murat, *C. R. Acad. Sci. Paris*, 303 series II(20) (1986) 1783.
- 15 M. Murat, D. Mathurin, M. Driouche and A. Bachiurrini, *Sci. Geol. Bull.*, 43 (1990) 213.
- 16 D. Mathurin, M.E. Chibi, and M. Murat, *Thermochim. Acta*, 98 (1986) 49.
- 17 P. R. Stuich, *J. Amer. Ceram. Soc.*, 69 (1986) 61.
- 18 S. Swier, G. Van Assche, A. Van Hemelrijck, H. Rahier, E. Verdonck and B. Van Mele, *J. Therm. Anal. Cal.*, 54 (1998) 585.